The speed of reaction–diffusion wavefronts in nonsteady media

2003 J. Phys. A: Math. Gen. 36 3983

(http://iopscience.iop.org/0305-4470/36/14/304)

INSTITUTE OF PHYSICS PUBLISHING JOURNAL OF PHYSICS A: MATHEMATICAL AND GENERAL

J. Phys. A: Math. Gen. **36** (2003) 3983–3993 PII: S0305-4470(03)55951-0

The speed of reaction–diffusion wavefronts in nonsteady media

Vicenç Méndez[1], **Joaquim Fort**[2] **and Toni Pujol**[2]

[1] Departament de Medicina, Facultat de Ciències de la Salut, Universitat Internacional de Catalunya. c/ Gomera s/n, 08190-Sant Cugat del Vallès (Barcelona), Spain
[2] Departament de Física, Universitat de Girona, Campus Montilivi, 17071 Girona, Catalonia, Spain

Received 6 November 2002, in final form 6 February 2003
Published 26 March 2003
Online at stacks.iop.org/JPhysA/36/3983

Abstract
The evolution of the speed of wavefronts for reaction–diffusion equations with time-varying parameters is analysed. We make use of singular perturbative analysis to study the temporal evolution of the speed for pushed fronts. The analogy with Hamilton–Jacobi dynamics allows us to consider the problem for pulled fronts, which is described by Kolmogorov–Petrovskii–Piskunov (KPP) reaction kinetics. Both analytical studies are in good agreement with the results of numerical solutions.

PACS numbers: 82.20.Fd, 05.40.Jc, 82.40.−g, 05.60.Cd

1. Introduction

Wavefronts are solutions to reaction–diffusion equations which travel without changing their shape. They appear in combustion [1], crystallization [2], superconductors [3], etc, and also have many biophysical applications (for a recent review, see [4]). Usually, one assumes that the reaction and diffusion parameters are uniform and steady. However, this may be a rough approximation to many systems, because both physical and biological media are, in general, nonuniform and time dependent. Many authors have considered the case of nonuniform media, by letting either the reduced reaction rate $a(x)$ or the diffusion coefficient $d(x)$ depend on position x [5–17]. However, the case of temporal dependences, namely $a(t)$ and $d(t)$, has remained apparently untackled. We will deal with this problem here. We will focus on the theoretical problem of determining the front speed. Specific applications will be the subject of future work. We would like to mention, however, that this problem can be very useful in biological applications such as population range expansions [18], for which the reproductive (i.e., reactive) and mobility (i.e., diffusive) parameters change in time driven by climatic changes. There are many additional examples of biological and physical systems [4] where the relevant parameters are time dependent because external factors make the density and/or

temperature change in time, e.g., in crystallization fronts, virus infections [19], forest fires [20] and models of the formation of Alzheimer's disease senile plaques [21].

We are thus interested in studying the dynamics of wavefront motion for the following problems:

$$\partial_t \rho = \partial_{xx}\rho + a(\varepsilon t) f(\rho) \qquad \partial_t \rho = d(\varepsilon t)\partial_{xx}\rho + f(\rho) \tag{1}$$

where, as usual [22], the function $f(\rho)$ satisfies $f(0) = f(1) = 0$. In equation (1), d and a are the dimensionless diffusion coefficient and reaction rate, respectively, and ε is a small parameter. We introduce an initial condition that may range from a step function ($\rho(x, 0) = 1$ for $x < 0$ and $\rho(x, 0) = 0$ for $x > 0$) to a fully developed wavefront. Since we expect solutions to behave like totally developed wavefronts, we should look at them in the asymptotic regime (large-space and large-time limit) by taking

$$t \to t/\varepsilon \qquad x \to x/\varepsilon. \tag{2}$$

The scaling considered is equivalent to assuming that the wavefront is totally developed independently of the way it developed from initial conditions. Equations (1) then become

$$\varepsilon\partial_t \rho = \varepsilon^2\partial_{xx}\rho + a(t) f(\rho) \qquad \varepsilon\partial_t \rho = \varepsilon^2 d(t)\partial_{xx}\rho + f(\rho). \tag{3}$$

Consistent with the initial conditions and the existence of a wavefront, we require the solution to satisfy $\lim_{x\to-\infty} \rho = 1$ and $\lim_{x\to\infty} \rho = 0$.

2. Non-KPP kinetics

In this section we make use of a singular perturbative analysis by taking ε as a small parameter to obtain the speed for pushed fronts in time-dependent media.

2.1. Nonsteady reaction rate

We consider the parabolic reaction–diffusion equation with a time-dependent reaction rate

$$\partial_t \rho = \partial_{xx}\rho + a(\varepsilon t) f(\rho) \qquad a(\varepsilon t) = 1 + \varepsilon\eta(\varepsilon t). \tag{4}$$

It is important to note that the perturbative method has no sense when $\eta(\varepsilon t) \gtrsim O(\varepsilon^{-1})$ because in this case the heterogeneity does not introduce a small (perturbative) correction but an important variation. This limitation will affect the particular results of the speed for growing temporal heterogeneities. After considering the hyperbolic scaling (2) one has from (4)

$$\varepsilon\partial_t \rho = \varepsilon^2\partial_{xx}\rho + a(t) f(\rho) \qquad a(t) = 1 + \varepsilon\eta(t) \tag{5}$$

under the boundary conditions $\lim_{x\to-\infty} \rho = 1$ and $\lim_{x\to\infty} \rho = 0$. We assume that the domain is divided into two regions according to the characteristic space scale of the field $\rho(x, t)$: a boundary layer region, whose width is $O(\varepsilon)$, in which ρ is rapidly varying; and an external region in which ρ is almost constant. In order to solve equation (5) in the outer region we expand ρ as follows:

$$\rho(x, t; \varepsilon) = \Psi_0(x, t) + \varepsilon\Psi_1(x, t) + \varepsilon^2\Psi_2(x, t) + O(\varepsilon^3). \tag{6}$$

By substituting (6) into (5) and collecting terms with the same powers of ε we get, for the lowest order, $f(\Psi_0) = 0$ under the boundary conditions $\lim_{x\to-\infty} \Psi_0 = 1$ and $\lim_{x\to\infty} \Psi_0 = 0$; for the first order $\partial_t \Psi_0 = f'(\Psi_0)\Psi_1 + \eta(t) f(\Psi_0)$ with $\lim_{x\to\pm\infty} \Psi_1 = 0$; and for the second order $\partial_t \Psi_1 = \partial_{xx}\Psi_0 + \frac{1}{2} f''(\Psi_0)\Psi_0^2 + f'(\Psi_0)\Psi_2 + \eta(t) f'(\Psi_0)\Psi_1$ with $\lim_{x\to\pm\infty} \Psi_2 = 0$. The solution for the lowest order is $\Psi_0 = 1$ to the left of the boundary

layer and $\Psi_0 = 0$ to the right of the boundary layer. The solutions for the following orders are $\Psi_i = 0$ $(i = 1, 2)$. Thus, $\rho(x, t; \varepsilon) = O(\varepsilon^3)$ to the right of the boundary layer and $\rho(x, t; \varepsilon) = 1 + O(\varepsilon^3)$ to the left of the boundary layer. Note that, up to the order of magnitude considered here, there is no effective difference between the time-independent media ($\varepsilon = 0$) case and the time-dependent media ($\varepsilon \neq 0$) case.

In order to study the dynamics in the interior of the boundary layer we translate equation (5) to the reference frame of the wavefront; i.e., we define the new variable $z = [x - S(t)]/\varepsilon$ where $S(t)$ represents the position of the wavefront. The derivatives in (3) transform according to

$$\partial_t \to -\frac{\dot{S}(t)}{\varepsilon}\partial_z + \partial_t \qquad \partial_{xx} \to \frac{1}{\varepsilon^2}\partial_{zz} \tag{7}$$

where the dot stands for the temporal derivative. We expand $\rho(z, t)$ and $S(t)$ in powers of ε

$$\rho(z, t) = \rho_0(z) + \varepsilon\rho_1(z, t) + \varepsilon^2\rho_2(z, t) + \cdots \qquad S(t) = S_0(t) + \varepsilon S_1(t) + \varepsilon^2 S_2(t) + \cdots \tag{8}$$

and, in consequence,

$$f(\rho) = f(\rho_0) + f'(\rho_0)\rho_1\varepsilon + \tfrac{1}{2}f''(\rho_0)\rho_1^2\varepsilon^2 + f'(\rho_0)\rho_2\varepsilon^2 + \cdots \tag{9}$$

where $f'(\rho_0) = \mathrm{d}f(\rho)/\mathrm{d}\rho|_{\rho=\rho_0}$. Inserting (8) and (9) into equation (5) once (7) are taken into account, and collecting terms with equal powers of ε one gets at $O(1)$, $O(\varepsilon)$ and $O(\varepsilon^2)$, respectively,

$$\mathcal{L}(\rho_0) = -f(\rho_0) \tag{10}$$

$$\mathcal{L}_1(\rho_1) = -f(\rho_0)\eta(t) - \dot{S}_1\partial_z\rho_0 \tag{11}$$

and

$$\mathcal{L}_1(\rho_2) = -\dot{S}_2\partial_z\rho_0 - \dot{S}_1\partial_z\rho_1 - \tfrac{1}{2}f''(\rho_0)\rho_1^2 - \eta(t)f'(\rho_0)\rho_1 + \partial_t\rho_1 \tag{12}$$

where $\mathcal{L} = \partial_{zz} + \dot{S}_0\partial_z$ and $\mathcal{L}_1 = \partial_{zz} + \dot{S}_0\partial_z + f'(\rho_0)$.

Since we assume $\rho_0 = \rho_0(z)$ then (10) is equivalent to the time-independent ($\varepsilon = 0$) parabolic reaction–diffusion equation translated to the wavefront reference frame ($z = x - \dot{S}_0 t$) which travels at constant speed $\dot{S}_0$. We call $\dot{S}_0 \equiv c$ and therefore $S_0 = ct$ where we assume $S(0) = 0$. From the solvability condition for the equation at each order of the expansion we will obtain the corresponding corrections to the speed of the wavefront. The solvability condition of (11) is $\int_{-\infty}^{\infty}\psi\mathcal{L}_1(\rho_1)\,\mathrm{d}z = 0$ [23], where ψ is such that $\mathcal{L}_1^\dagger(\psi) = 0$, $\mathcal{L}_1^\dagger = \partial_{zz} - \dot{S}_0\partial_z + f'(\rho_0)$ being the adjoint operator of $\mathcal{L}_1$ [23]. It is easy to show that $\psi = \mathrm{e}^{cz}\,\mathrm{d}\rho_0/\mathrm{d}z$ is an eigenfunction of $\mathcal{L}_1^\dagger$ with null eigenvalue. The solvability condition for (11) may be written as

$$\int_{-\infty}^{\infty}\mathrm{e}^{cz}\frac{\mathrm{d}\rho_0}{\mathrm{d}z}\left[-f(\rho_0)\eta(t) - \dot{S}_1\frac{\mathrm{d}\rho_0}{\mathrm{d}z}\right]\mathrm{d}z = 0 \tag{13}$$

so that

$$\dot{S}_1 = -\frac{\eta(t)\int_{-\infty}^{\infty}\mathrm{e}^{cz}\frac{\mathrm{d}\rho_0}{\mathrm{d}z}f(\rho_0)\,\mathrm{d}z}{\int_{-\infty}^{\infty}\mathrm{e}^{cz}\left(\frac{\mathrm{d}\rho_0}{\mathrm{d}z}\right)^2\mathrm{d}z}. \tag{14}$$

The integral in the numerator of (14) may be simplified by using (10) and integrating by parts:

$$\begin{aligned}\int_{-\infty}^{\infty}\mathrm{e}^{cz}\frac{\mathrm{d}\rho_0}{\mathrm{d}z}f(\rho_0)\,\mathrm{d}z &= -\int_{-\infty}^{\infty}\mathrm{e}^{cz}\frac{\mathrm{d}\rho_0}{\mathrm{d}z}\frac{\mathrm{d}^2\rho_0}{\mathrm{d}z^2}\,\mathrm{d}z - c\int_{-\infty}^{\infty}\mathrm{e}^{cz}\left(\frac{\mathrm{d}\rho_0}{\mathrm{d}z}\right)^2\mathrm{d}z \\ &= -\frac{1}{2}c\int_{-\infty}^{\infty}\mathrm{e}^{cz}\left(\frac{\mathrm{d}\rho_0}{\mathrm{d}z}\right)^2\mathrm{d}z.\end{aligned}$$

Finally one can obtain the first correction to the speed

$$\dot{S}_1 = \tfrac{1}{2} c\eta(t). \tag{15}$$

Note that in (15) there is no dependence on the solution of ρ_0 but only on the function η.

Before proceeding with the following order in the expansion, it is necessary to solve (11). As $\mathcal{L}_1(\mathrm{d}\rho_0/\mathrm{d}z) = 0$ we look for a solution of the form $\rho_1(z,t) = \frac{\mathrm{d}\rho_0}{\mathrm{d}z} + \frac{\mathrm{d}\rho_0}{\mathrm{d}z} zF(t)$ into (11), finding that $F(t) = \frac{1}{2}\eta(t)$. Thus

$$\rho_1(z,t) = \frac{\mathrm{d}\rho_0}{\mathrm{d}z}\left[1 + \frac{1}{2}\eta(t)z\right]. \tag{16}$$

After substituting $S_0 = ct$, (15) and (16) into (12) and applying the solvability condition [23] $\int_{-\infty}^{\infty} \mathrm{e}^{cz}\frac{\mathrm{d}\rho_0}{\mathrm{d}z}\mathcal{L}_1(\rho_2)\,\mathrm{d}z = 0$ for (12) we get

$$\dot{S}_2 = -\frac{c}{8}\eta(t)^2 + \alpha\dot{\eta}(t) \tag{17}$$

where

$$\alpha = \frac{1}{2}\frac{\int_{-\infty}^{\infty} z\,\mathrm{e}^{cz}\left(\frac{\mathrm{d}\rho_0}{\mathrm{d}z}\right)^2 \mathrm{d}z}{\int_{-\infty}^{\infty}\mathrm{e}^{cz}\left(\frac{\mathrm{d}\rho_0}{\mathrm{d}z}\right)^2 \mathrm{d}z}. \tag{18}$$

Note that in this case $\dot{S}_2$ depends explicitly on the solution of ρ_0. In order to compute analytically the second-order correction to the speed, it is necessary to have an analytical expression for the zeroth-order solution $\rho_0(z)$. Some exact solutions are known [24] for reaction terms of the form

$$f(\rho) = \rho^{q+1}(1-\rho^q) \tag{19}$$

with $q \geqslant 1$. This source term has been applied to forest fires [20, 22] and the spread of microorganisms [25]. In this case, the solution for the lowest-order equation takes the form

$$\rho_0(z) = \frac{1}{(1+\mathrm{e}^{bz})^{\sigma}} \qquad c = \frac{1}{\sqrt{1+q}} \qquad b = qc \qquad \sigma = \frac{1}{q}.$$

It is easy to check that the integrals involved in (18) are convergent for any q. For example, for $q = 1$ we have $f(\rho) = \rho^2(1-\rho), \alpha = \frac{3}{4}\sqrt{2}, c = \frac{1}{\sqrt{2}}$ and the speed of the wavefront is given by

$$v(t) = \frac{1}{\sqrt{2}} + \frac{1}{2\sqrt{2}}\eta(t)\varepsilon + \left[\frac{3}{4}\sqrt{2}\dot{\eta}(t) - \frac{1}{8\sqrt{2}}\eta(t)^2\right]\varepsilon^2 + O(\varepsilon^3). \tag{20}$$

If we choose $\eta(t) = t$ and $f(\rho) = \rho^2(1-\rho)$ one has, after inverting the hyperbolic scaling

$$v(t) = \frac{1}{\sqrt{2}} + \left(\frac{t}{2\sqrt{2}} + \frac{3\sqrt{2}}{4}\right)\varepsilon^2 + \cdots. \tag{21}$$

Note that the first term in brackets is a secular term and (21) fails to be valid at $t \sim O(\varepsilon^{-2})$. In figure 1 we compare the results of the numerical integrations of equations (4) and (19) with $q = 1$ (open symbols) with the analytical prediction given by equation (21) (solid lines) for $\varepsilon^2 = 0.005$ and $\varepsilon^2 = 0.01$. There is good agreement between (21) and the speed observed in the numerical simulations. This confirms the validity of our approach given above. However (21) is only valid up to $t \sim \varepsilon^{-2}$. This is the reason why the theoretical prediction for $\varepsilon^2 = 0.01$ in figure 1 begins to disagree for $t \sim 100$ with the numerical results. If one chooses a time-decaying function and initially bounded for $\eta(t)$ (for instance $\eta(t) = \mathrm{e}^{-t}$) in (20) then the problem of secular terms will not appear.

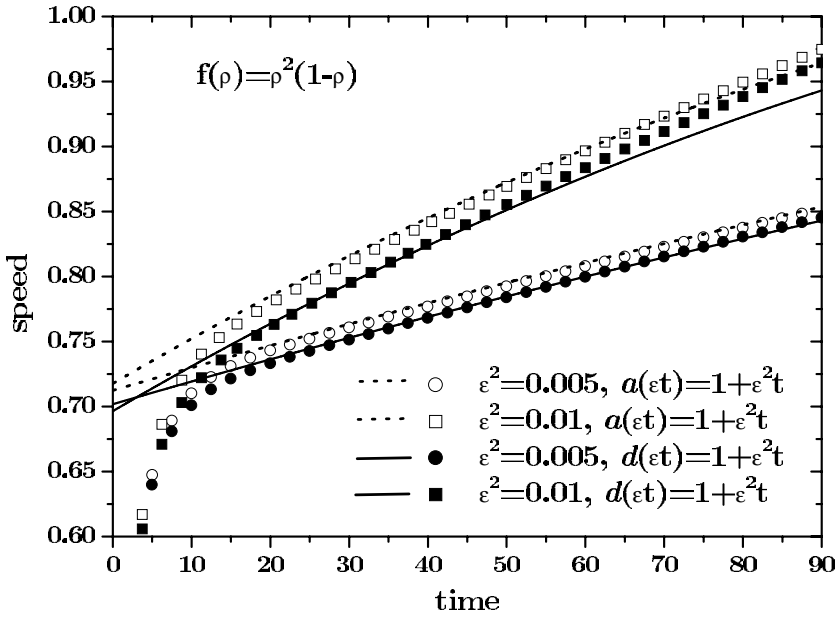

Figure 1. Temporal evolution of the speed of wavefronts for $f(\rho) = \rho^2(1-\rho)$. Here we analyse two different cases of weakly nonsteady media: (i) reaction rate a (open symbols) and (ii) diffusion coefficient d (filled symbols) linearly increasing with time. The analytical predictions, given by equations (21) and (27), are plotted as dotted and solid lines, respectively. The speeds observed in numerical integrations of equations (1), with an initial step function $\rho(x, t = 0)$, are plotted as symbols. There is a good agreement between our new formulae and the simulations.

2.2. Nonsteady diffusion coefficient

In this section, we start with the problem

$$\partial_t \rho = d(\varepsilon t)\partial_{xx}\rho + f(\rho) \qquad d(\varepsilon t) = 1 + \varepsilon\zeta(\varepsilon t). \tag{22}$$

As in the previous section, the perturbative method has no sense when $\zeta(\varepsilon t) \gtrsim O(\varepsilon^{-1})$. After considering the hyperbolic scaling (2) we have

$$\varepsilon\partial_t \rho = d(t)\varepsilon^2\partial_{xx}\rho + f(\rho) \qquad d(t) = 1 + \varepsilon\zeta(t) \tag{23}$$

under the boundary conditions $\lim_{x\to-\infty}\rho = 1$ and $\lim_{x\to\infty}\rho = 0$.

In order to solve equation (23) in the outer region we use the expansion (6). As in the previous section $\rho(x, t; \varepsilon) = O(\varepsilon^3)$ and to the right of the boundary layer and $\rho(x, t; \varepsilon) = 1 + O(\varepsilon^3)$ to the left of the boundary layer. To study the dynamics of (23) inside the boundary layer we substitute (7), (8) and (9) into (23) and collect terms with equal powers of ε. We finally find (10) and

$$\mathcal{L}_1(\rho_1) = -\zeta(t)\partial_{zz}\rho_0 - \dot{S}_1\partial_z\rho_0 \tag{24}$$

and

$$\mathcal{L}_1(\rho_2) = -\dot{S}_2\partial_z\rho_0 - \dot{S}_1\partial_z\rho_1 - \tfrac{1}{2}f''(\rho_0)\rho_1^2 - \zeta(t)\partial_{zz}\rho_1 + \partial_t\rho_1. \tag{25}$$

for first and second orders, respectively. From the solvability conditions and assuming $\rho_0 = \rho_0(z)$ one has $\dot{S}_0 = c$ constant and

$$\dot{S}_1 = \frac{1}{2}c\zeta(t) \qquad \dot{S}_2 = -\frac{c}{8}\zeta(t)^2 - \alpha\dot{\zeta}(t) \qquad \rho_1(z,t) = \frac{\mathrm{d}\rho_0}{\mathrm{d}z}\left[1 - \frac{1}{2}\zeta(t)z\right]$$

where α is given in (18). If we choose $f(\rho) = \rho^2(1-\rho)$ one has

$$v(t) = \frac{1}{\sqrt{2}} + \frac{1}{2\sqrt{2}}\zeta(t)\varepsilon + \left[-\frac{3}{4}\sqrt{2}\dot{\zeta}(t) - \frac{1}{8\sqrt{2}}\zeta(t)^2\right]\varepsilon^2 + O(\varepsilon^3) \tag{26}$$

and introducing $\zeta(t) = t$, after inverting the hyperbolic scaling, one gets

$$v(t) = \frac{1}{\sqrt{2}} + \left(\frac{t}{2\sqrt{2}} - \frac{3\sqrt{2}}{4}\right)\varepsilon^2 + \cdots. \tag{27}$$

In figure 1 we also show the comparison between (27) with the numerical integrations of equation (22) (filled symbols). Again, there is a good agreement between the theoretical result and the speeds observed in the numerical simulations but (27) fails to be valid at $t \sim O(\varepsilon^{-2})$ as occurs in the previous case.

3. KPP kinetics

We stress that singular perturbation analysis does not yield a fully analytical result for the very important Kolmogorov–Petrovskii–Piskunov (KPP) kinetics (pulled fronts), i.e. $f(\rho) = \rho(1-\rho)$ [18, 19, 24], if one needs to go beyond first order in ε, because the exact solution for (10) is unknown. In this section we determine the temporal evolution of the position of the reaction wavefront for the logistic case. We start from the first of equations (3) but an analogous analysis may be done for the second one:

$$\varepsilon\partial_t\rho^\varepsilon = \varepsilon^2\partial_{xx}\rho^\varepsilon + a(t)\rho^\varepsilon(1-\rho^\varepsilon) \tag{28}$$

where $\rho^\varepsilon(x,t) = \rho(x/\varepsilon, t/\varepsilon)$, and we replace $\rho^\varepsilon(x,t)$ by an auxiliary field $G^\varepsilon(x,t) \geqslant 0$ through the exponential (WKB) transformation

$$\rho^\varepsilon(x,t) = \mathrm{e}^{-G^\varepsilon(x,t)/\varepsilon} \tag{29}$$

where $G^\varepsilon(x,t)$ has to be found. It follows from (29) that $\rho^\varepsilon(x,t) \to 0$ as $\varepsilon \to 0$ and the boundary of the set $G(x,t) > 0$, where $G(x,t) = \lim_{\varepsilon\to 0} G^\varepsilon(x,t)$, determines the position of the wavefront [26]. Therefore, the position of the front can be determined by the equation $G(x(t),t) = 0$. Inserting (29) into (28) one has

$$\partial_t G^\varepsilon + (\partial_x G^\varepsilon)^2 - \varepsilon\partial_{xx}G^\varepsilon + a(t)\left(1 - \mathrm{e}^{-G^\varepsilon/\varepsilon}\right) = 0. \tag{30}$$

By considering the limit $\varepsilon \to 0$, since $\lim_{\varepsilon\to 0} \mathrm{e}^{-G^\varepsilon/\varepsilon} = 0$ provided $G^\varepsilon(x,t) > 0$, it follows from (30) that $G(x,t)$ obeys the Hamilton–Jacobi equation

$$\partial_t G + (\partial_x G)^2 + a(t) = 0. \tag{31}$$

It is important to note that if $f(\rho)$ in non-KPP, for example $f = \rho^2(1-\rho)$, the last term on the left-hand side of (30) becomes $a(t)\,\mathrm{e}^{-G^\varepsilon/\varepsilon}\left(1 - \mathrm{e}^{-G^\varepsilon/\varepsilon}\right)$ and taking $\varepsilon \to 0$ this term vanishes and one loses the information related to the reaction process. Therefore the Hamilton–Jacobi method does not hold when the linearization of $f(\rho)$ near the unstable state ($\rho = 0$) is zero (pushed fronts).

Following the same steps as before but for the time-dependent diffusion coefficient, one has alternatively

$$\partial_t G + d(t)\,(\partial_x G)^2 + 1 = 0. \tag{32}$$

From the analogy with the general form of the Hamilton–Jacobi equation $\partial_s G + H(\partial_x G, s) = 0$ one finds the Hamiltonian $H(p,s)$ where we call s the temporal coordinate and $p = \partial_x G$. The solution of the Hamilton–Jacobi equation is, as in classical mechanics,

$$G(x,t) = \min_{x(s=0)=0, x(s=t)=x} \int_0^t L[x(s),\, p(s)]\,\mathrm{d}s \tag{33}$$

where $L[x(s), p(s)] = p(s)\dot{x}(s) - H$ is the Lagrangian function and $x(s)$ and $p(s)$ must be found from the Hamilton equations $\dot{x}(s) = \partial_p H$ and $\dot{p}(s) = -\partial_x H$ under the boundary conditions $x(0) = 0$ and $x(t) = x$.

3.1. Nonsteady reaction rate

In this case one has $\dot{x}(s) = 2p$ where p is constant and the solution is $x(s) = xs/t$. Finally, the Lagrangian function is

$$L = \frac{x^2}{4t^2} - a(s)$$

and the solution for the function $G(x, t)$ from (33) is

$$G(x, t) = \frac{x^2}{4t^2} - \int_0^t a(s)\,\mathrm{d}s$$

so that the position of the wavefront is given by

$$x(t) = 2\left[t\int_0^t a(s)\,\mathrm{d}s\right]^{1/2} \tag{34}$$

and the speed of the wavefront is

$$v(t) = \frac{ta(t) + \int_0^t a(s)\,\mathrm{d}s}{\left[t\int_0^t a(s)\,\mathrm{d}s\right]^{1/2}}. \tag{35}$$

We again consider the important case of weak time-dependent media, namely $a(\varepsilon t) = 1 + \varepsilon^2 t$, which yields

$$v(t) = \frac{2 + 3\varepsilon^2 t/2}{\sqrt{1 + \varepsilon^2 t/2}} \tag{36}$$

after inverting the hyperbolic scaling. From figure 2, we see that for $\varepsilon^2 = 0.005$ and $\varepsilon^2 = 0.01$ this result is also confirmed by the numerical simulations.

3.2. Nonsteady diffusion coefficient

From (32) the Hamilton function for this case is given by

$$H = d(s)p^2 + 1$$

and from the Hamilton equations one has $\dot{x}(s) = 2pd(s)$, which has the solution

$$x(s) = \frac{\int_0^s d(s')\,\mathrm{d}s'}{\int_0^t d(s')\,\mathrm{d}s'}x$$

after using $x(0) = 0$ and $x(t) = x$. Finally, the Lagrangian function is

$$L = \frac{x^2}{4\left[\int_0^t d(s')\,\mathrm{d}s'\right]^2}\,d(s) - 1$$

and

$$G(x, t) = \frac{x^2}{4\int_0^t d(s')\,\mathrm{d}s'} - t.$$

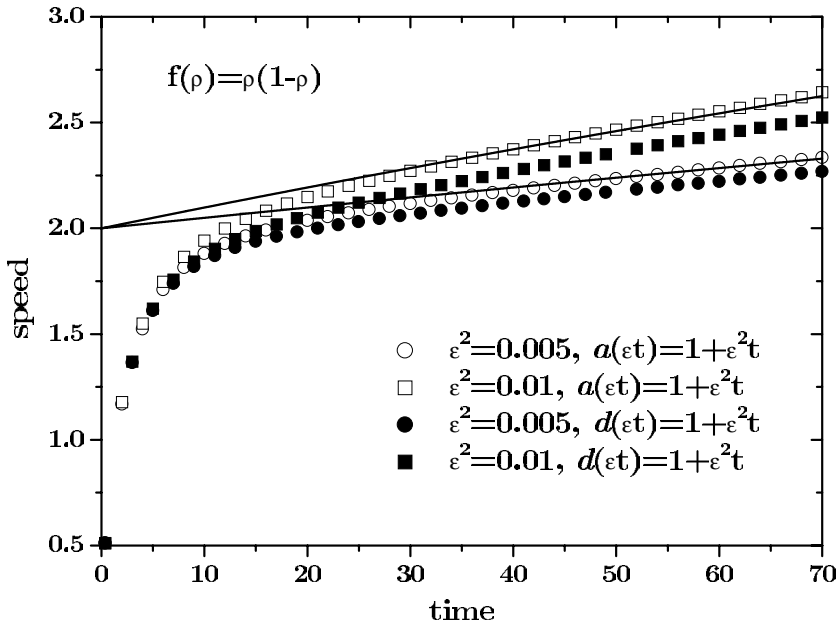

Figure 2. Temporal evolution of the speed of wavefronts for logistic growth, i.e. $f(\rho) = \rho(1-\rho)$. As in figure 1, we include two different cases of weakly nonsteady media: (i) reaction rate $a(\varepsilon t)$ (open symbols) and (ii) diffusion coefficient $d(\varepsilon t)$ (filled symbols) linearly increasing with time. The analytical predictions, given by equation (36), are plotted as solid lines. Speeds from numerical integrations of equations (1), using a step function for $\rho(x, 0)$, are plotted as symbols. In contrast to figure 1, the analytical solutions are based on Hamilton–Jacobi dynamics because the perturbation method of section 2 cannot be applied to this $f(\rho)$, which is however very useful in biophysical applications [18, 19].

The position of the wavefront is then

$$x(t) = 2\left[t\int_0^t d(s')\,\mathrm{d}s'\right]^{1/2}. \tag{37}$$

From this result we conclude that the problems

$$\partial_t\rho = \partial_{xx}\rho + g(\varepsilon t)\rho(1-\rho) \qquad \partial_t\rho = g(\varepsilon t)\partial_{xx}\rho + \rho(1-\rho)$$

have the same speed given by

$$v(t) = \frac{\varepsilon t g(\varepsilon t) + \int_0^{\varepsilon t} g(s)\,\mathrm{d}s}{\left[\varepsilon t\int_0^{\varepsilon t} g(s)\,\mathrm{d}s\right]^{1/2}}$$

in the limit $\varepsilon \to 0$ (large-time limit). Note that this does not occur for non-KPP kinetics, since there is a sign difference between (21) and (27).

In figure 2 we have compared numerical versus analytical solutions. There is good agreement, which confirms the validity of the formulae derived above. From figures 1 and 2 we see that for linearly increasing functions $a(t)$ and/or $d(t)$ the reaction–diffusion wavefront is accelerated, as was to be expected intuitively. However, we are not aware of any paper where this problem has been tackled previously.

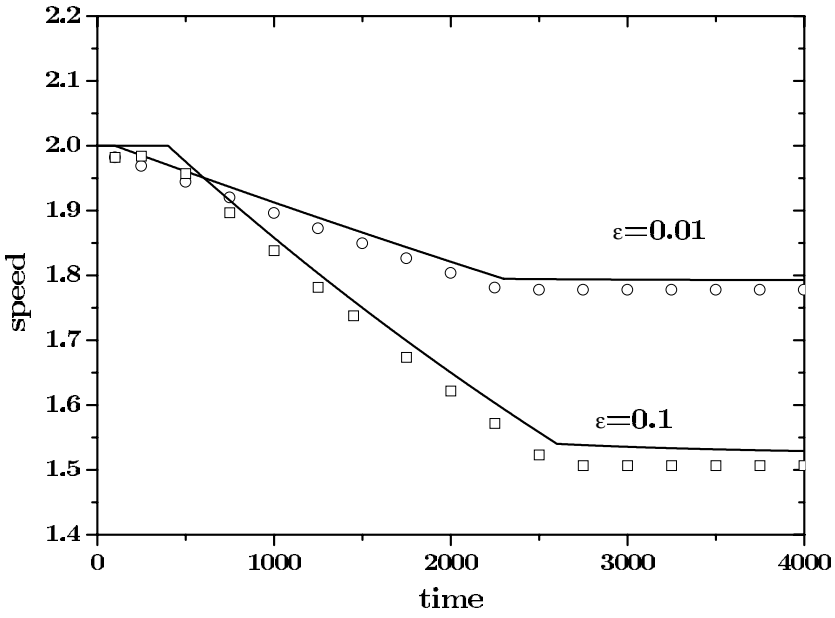

Figure 3. Temporal evolution of the speed of wavefronts for an exponentially decaying reaction rate (or, alternatively, an exponentially decaying diffusion coefficient: both cases give the same speed for KPP kinetics) and $f(\rho) = \rho(1-\rho)$. Here we have used $t^* = 100, t^{**} = 2300$ for $\varepsilon = 0.01$; and $t^* = 400, t^{**} = 2600$ for $\varepsilon = 0.1$. The analytical solution given by equation (40) has been plotted as solid lines. Symbols correspond to the results from numerical simulations of equations (1) with (38) taking an initial step function for $\rho(x, 0)$. The wavefront slows down in a way consistent with our new analytical result.

3.3. Nonlinear systems

Finally, we would like to mention that the usefulness of our methods is not restricted to the relevant case of linear-varying time-dependent parameters. This point may be rather important in practice because, in some cases, the parameter values of the media may change fast enough so as to invalidate linear approximations for $a(t)$ and $d(t)$ in the timescale typical of the wavefront speed measurements. This is why we have also checked our analytical results, again by means of numerical solutions, for the example of a reaction rate which diminishes according to

$$a(\varepsilon t) = \begin{cases} 1 & 0 < t < t^* \\ \exp\left(-\varepsilon \dfrac{t - t^*}{t^*}\right) & t^* < t < t^{**} \\ \exp\left(-\varepsilon \dfrac{t^{**} - t^*}{t^*}\right) = \text{constant} & t > t^{**}. \end{cases} \tag{38}$$

Making use of equation (2) in (38) and computing the wavefront position from equation (34) one has

$$x^2(t) = \begin{cases} 4t^2 & 0 < t < \varepsilon t^* \\ 4t\left[\varepsilon t^* + t^*\left(1 - \mathrm{e}^{-\frac{t-\varepsilon t^*}{t^*}}\right)\right] & \varepsilon t^* < t < \varepsilon t^{**} \\ 4t\left[\varepsilon t^* + t^*\left(1 - \mathrm{e}^{-\varepsilon\frac{t^{**}-t^*}{t^*}}\right) + (t - \varepsilon t^{**})\,\mathrm{e}^{-\varepsilon\frac{t^{**}-t^*}{t^*}}\right] & t > \varepsilon t^{**}. \end{cases} \tag{39}$$

In order to calculate the analytical solution for the speed we take $\mathrm{d}x(t)/\mathrm{d}t$ and invert the hyperbolic scaling. This finally yields

$$v(t) = \begin{cases} 2 & 0 < t < t^* \\ \dfrac{\varepsilon t^* + t^*\left(1 - \mathrm{e}^{-\varepsilon\frac{t-t^*}{t^*}}\right) + \varepsilon t\,\mathrm{e}^{-\varepsilon\frac{t-t^*}{t^*}}}{\left\{\varepsilon t\left[\varepsilon t^* + t^*\left(1 - \mathrm{e}^{-\varepsilon\frac{t-t^*}{t^*}}\right)\right]\right\}^{1/2}} & t^* < t < t^{**} \\ \dfrac{\varepsilon t^* + t^*\left(1 - \mathrm{e}^{-\varepsilon\frac{t^{**}-t^*}{t^*}}\right) + \varepsilon(2t - t^{**})\,\mathrm{e}^{-\varepsilon\frac{t^{**}-t^*}{t^*}}}{\left\{\varepsilon t\left[\varepsilon t^* + t^*\left(1 - \mathrm{e}^{-\varepsilon\frac{t^{**}-t^*}{t^*}}\right) + \varepsilon(t - t^{**})\,\mathrm{e}^{-\varepsilon\frac{t^{**}-t^*}{t^*}}\right]\right\}^{1/2}} & t > t^{**}. \end{cases} \tag{40}$$

These results have been plotted in figure 3 and compared to numerical simulations. We observe, once again, a very good agreement. Therefore, our method can also be used to derive wavefront speeds in nonlinear evolving media. An analogous analysis could be performed for non-KPP kinetics by using singular perturbative analysis with nonlinear time-dependent reaction rate and/or diffusion coefficient with the structure given by (4) and (22). However, we do not include the calculations for the sake of brevity.

4. Conclusions

In many reaction–diffusion systems, the relevant parameters may vary in time. Here, we have presented two theoretical approaches to determine the speed of wavefronts as a function of time: a perturbative approach (valid for non-KPP kinetics, figure 1), and another one based on Hamilton–Jacobi dynamics (valid for KPP kinetics, figure 2). In all cases, there is good agreement between the theoretical prediction and the results from direct numerical integrations of the reaction–diffusion equation. Our approach can also be applied to non-weakly time-dependent media, i.e. to the case in which the relevant parameter values do not evolve linearly in time (figure 3). Specific applications will be the subject of future work.

Acknowledgments

Computing equipment used has been funded in part by the CICYT of the Ministry of Science and Technology under grants BFM 2000-0351 and SGR-2001-00186 (VM and JF) and REN 2000-1621 CLI (JF and TP).

References

[1] Fort J, Pujol T and Cukrowski A S 2000 *J. Phys. A: Math. Gen.* **33** 6953
[2] Herlach D M 1994 *Mater. Sci. Eng.* R **12** 177
[3] Di Bartolo S J and Dorsey A T 1996 *Phys. Rev. Lett.* **77** 4442
[4] Fort J and Méndez V 2002 *Rep. Prog. Phys.* **65** 895
[5] Sendiña-Nadal I *et al* 1997 *Phys. Rev.* E **56** 6298
[6] Steinbock O, Zykov V S and Müller S C 1993 *Phys. Rev.* E **48** 3295
[7] Shebesch I and Engel H 1998 *Phys. Rev.* E **57** 3905
[8] Xin J 2000 *SIAM Rev.* **42** 161
[9] Shigesada N 1986 *Theor. Popul. Biol.* **30** 143
[10] Nakamura K I, Matano H, Hilhorst D and Schätzle R 1999 *J. Stat. Phys.* **95** 1165
Norbury J and Yeh L C 2001 *Nonlinearity* **14** 849
Norbury J and Yeh L C 2001 *SIAM J. Appl. Math.* **61** 1418
[11] Keener J P 2000 *Physica* D **136** 1
[12] Keener J P 2000 *Siam J. Appl. Math.* **61** 317
[13] Bugrim A, Zhabotinsky A and Epstein I 1997 *Biophys. J.* **73** 2897
[14] Mitkov I, Kladko K and Pearson J E 1998 *Phys. Rev. Lett.* **81** 5453

[15] Rotstein H G, Zhabotinsky A M and Epstein I R 2001 *Chaos* **11** 833
[16] Ponce Dawson S, Keizer J and Pearson J E 1999 *Proc. Natl Acad. Sci. USA* **96** 6060
[17] Petrovskii S V 1993 *Tech. Phys. Lett.* **19** 397
[18] Fort J and Méndez V 1999 *Phys. Rev. Lett.* **82** 867
Fort J and Méndez V 1999 *Phys. Rev.* E **60** 5894
[19] Fort J and Méndez V 2002 *Phys. Rev. Lett.* **89** 178101
[20] Méndez V and Llebot J E 1997 *Phys. Rev.* E **56** 6557
[21] Edelsten-Keshet L and Spiros A 2002 *J. Theor. Biol.* **216** 301
[22] Méndez V, Fort J and Farjas J 1999 *Phys. Rev.* E **60** 5231
[23] Evans L C 1998 *Partial Differential Equations* (Providence, RI: American Mathematical Society)
[24] Murray J D 1989 *Mathematical Biology* (Berlin: Springer)
[25] Vereecken K M, Dens E J and Van Impe J F 2000 *J. Theor. Biol.* **205** 53
[26] Fedotov S 1999 *Phys. Rev.* E **59** 5040
Fedotov S 1998 *Phys. Rev.* E **58** 5143